

Tuning of an Integrated Tunable Laser for Swept Source Optical Coherence Tomography

Rastko Pajković, Kevin Williams and Erwin Bente

Photonic Integration Group, Department of Electrical Engineering, Eindhoven University of Technology,
PO Box 513, 5600 MB Eindhoven, The Netherlands.

r.pajkovic@tue.nl

A recent widely tunable integrated semiconductor laser design shows promise in answering the needs for a swept source optical coherence tomography source. A wavelength sweep linear in frequency remains to be demonstrated. We present preliminary results of tuning and discuss the wavelength calibration.

Introduction

Swept source optical coherence tomography (OCT) requires a source that can perform sweeps at 50 kHz or faster, linear in frequency, across a wavelength range wider than 100 nm [1]. To accommodate the anticipated advances in OCT – multimodality and parallelization, an ideal source should also be compact and low cost. A novel 1.5 μm widely tunable semiconductor laser that can potentially meet these requirements was recently developed in our group [2]. This laser, which is realized as a photonic integrated circuit on InP, has an advantage over the existing solutions that stems from its tuning mechanism. This mechanism is based on a reverse biased phase modulator that does not dissipate heat (typical electrical power dissipation in the order of 1 μW) as opposed to current-controlled gratings, such as distributed Bragg reflectors (DBR). This in turn provides better wavelength stability since the thermal equilibrium in the filter does not change. This is especially relevant around the points in the scan where the control signals applied to the tunable filter in the laser need to be changed discontinuously. While a wide tuning range of 74 nm was achieved with the existing design, a linear sweep with steps in the order of 5 GHz remains to be demonstrated. In this paper we discuss the laser operation principle, propose a calibration routine for performing a linear sweep in frequency and present preliminary results of tuning.

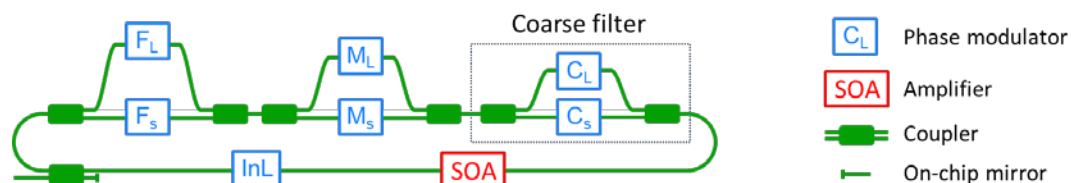


Figure 1 Schematic of the ring laser cavity, displaying 7 phase modulators, and a semiconductor optical amplifier (SOA) that is biased at a constant current. Phase modulators are named according to the filter that they belong to - F(ine), M(edium) and C(oarse), S and L in the index stand for short and long arm, respectively. InL stands for in-line phase modulator, that is used to control the cavity mode position. The on-chip mirror strongly favors one lasing direction over the other, and ensures unidirectional lasing.

Lasing wavelength is selected by tuning three asymmetric Mach-Zehnder interferometers (AMZI) in series as depicted in Figure 1. Each AMZI is a periodic spectral filter with a sinusoidal transmission spectrum. The three filters provide coarse, medium and fine tuning. The filter's peak transmission is controlled by controlling the voltage applied to

the phase modulator (PM) within the filter. To achieve a sweep linear in frequency, all three filters' peak transmission points need to be aligned and tuned synchronously. The position of the cavity mode can be fine-tuned using an additional phase modulator (indicated in Figure 1 as InL which stands for in-line phase modulator).

Targeted sweep parameters

A typical OCT sweep consists of 1000 to 2000 sampling points, that ideally correspond to equidistant lasing frequencies. The free spectral range of our laser is 5.2 GHz at 1530 nm, see Table 1. Longitudinal cavity modes offer a natural frequency comb that, over a tuning range of 74 nm, provides 1855 frequency references. Our goal is to achieve a stepwise sweep with a spacing of approximately 5 GHz between subsequent points, utilizing the cavity mode spacing, across the entire tuning range of 74 nm. To be able to achieve a reliable and reproducible sweep we need to characterize the response of each phase modulator (in phase and amplitude) inside the cavity and establish the imbalance in the AMZIs as a function of wavelength. With that information we can build a model to predict the laser output wavelength and quality as a function of the control voltages.

Methodology

Due to the variation in phase modulators from different fabrication runs [3] and even wafer locations, the phase delay as a function of voltage of different phase modulators can vary significantly. To characterize the response of the phase modulators inside the cavity, we use two approaches: we measure the laser output spectrum when lasing and below threshold. Measurements when lasing provide an accurate value of the lasing wavelength. This is the wavelength of the cavity mode that has the lowest loss determined by the filter system in combination with the gain profile of the amplifying medium. Although accurate in terms of lasing wavelength, measuring when lasing gives little information of the individual contributions of the coarse, medium and fine filters. This is due to the fact that the non-lasing modes are suppressed and the effect of the transfer function of the filter system at wavelengths other than the lasing wavelength becomes less prominent. For this reason we also perform subthreshold measurements which allow us to observe the transfer function of the filter system in more detail. These measurements should provide data for modelling the laser. Subthreshold measurements do not provide an accurate prediction of the lasing wavelength (for the same filter settings at $I_{SOA} > I_{th}$) because a change in the bias current influences the chip temperature, gain profile [4] and the refractive index of the amplifying medium, which all influence the lasing wavelength.

Measurements

The laser under test is enclosed in a package and thermally stabilized at 18°C for all measurements. Subthreshold measurements are performed at a constant bias current $I_{SOA} = 65$ mA and lasing measurements are performed at $I_{SOA} = 150$ mA. For recording the laser spectrum Ando AQ-6315A was used, with a resolution of 0.05 nm and minimal sample spacing of 0.01 nm, that can just resolve the cavity modes. All measurements start with all phase modulators biased at 0 V, the change in output spectrum is monitored when changing the reverse bias voltage of a single modulator in equidistant steps.

First we have characterized the response of the in-line phase modulator subthreshold, see Figure 2(a). This measurement shows that the influence of the in-line modulator on the peak wavelength is small, in the order of the cavity mode spacing at most. Additionally,

the reverse bias has a notable influence on the absorption of the phase modulator, as peak power drops by more than 15 dB. Closer inspection reveals that the effect is more pronounced at higher voltages, that should therefore be avoided during operation. It appears that the absorption is wavelength dependent and that it decreases when the phase modulator is biased from 0 to 1 V. This result calls for further investigation of the effect, in a phase modulator outside of the cavity.

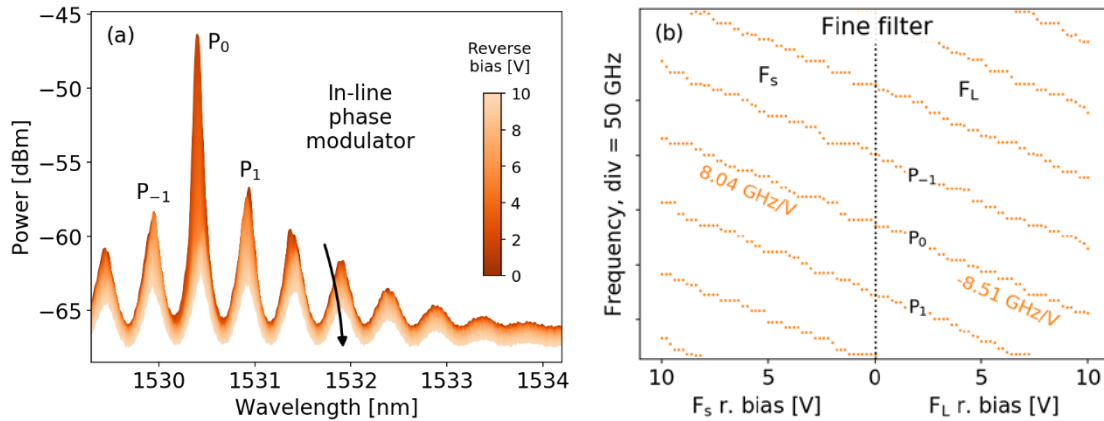


Figure 2 Subthreshold measurement results for $I_{SOA} = 65$ mA. (a) Change in spectrum when in-line phase modulator is tuned and (b) change in peak frequency when the F_s and F_b phase modulators of the fine filter are tuned. Peaks are labeled with P_x with the most prominent peak being P_0 .

Figure 2(b) shows how the peak positions change when both phase modulators from the fine filter are tuned sequentially. In figures (a) and (b) peak labels P_{-1} , P_0 and P_1 from correspond to the same peaks, when all phase modulators are biased at 0 V. Peaks appear to shift linearly with the modulator bias, with jumps of 0.04 nm on average. The jump step corresponds to the cavity mode spacing, see Table 1. Otherwise, linearity of the peak frequency is in line with the phase modulator model which shows that the phase changes linearly with bias voltage [3]. The fine filter response in GHz/V is shown in Figure 2(b) for peak P_0 . The response is given by the slope of a linear fit, with the standard error of the slopes being 0.12 GHz/V and 0.10 GHz/V for the short arm and long arm, respectively. This measurement shows that there is variation between two different PM responses.

Table 1 Filter design parameters, derived and measured properties.

* Average cavity length, where the filter length is taken as the average length of the arms.

** Average slope (linear fit, least sum of squares) of 7 measured peaks, P_{-3} to P_3

*** Calculated for $n_g = 3.67$ at 1530nm, taken from [5].

Filter	Arm mismatch [μm]	FSR*** [nm]	FSR*** [GHz]	Response (est.) [GHz/V]	Response (meas.) [GHz/V]
Coarse	8	79.3	10 210.9	850.9	
Medium	90	7.09	907.6	75.6	
Fine	1 263	0.50	64.5	5.4	8.25**
Cavity	15 550*	0.04	5.2		

In calculating the free spectral range (FSR) shown in Table 1, the following group refractive index measurements [5] were used:

$$n_g^{\text{shallow}} = 3.658 + 0.900 \cdot (1.53 - \lambda[\mu\text{m}])$$

$$n_g^{\text{deep}} = 3.674 + 0.843 \cdot (1.53 - \lambda[\mu\text{m}])$$

where deep and shallow stand for deep and shallow trench [6].

Finally we measure the response of the medium filter under lasing conditions, seen in Figure 3(a), which allows us to estimate the filter response. The same is done for the coarse filter not shown here, and the results are used to match the responses of the two filters and tune them synchronously. Results of synchronous tuning of the coarse and medium filters are seen in Figure 3(b). A tuning range of 40 nm is achieved, with undesired mode hops, which indicate that a more accurate measurement is necessary.

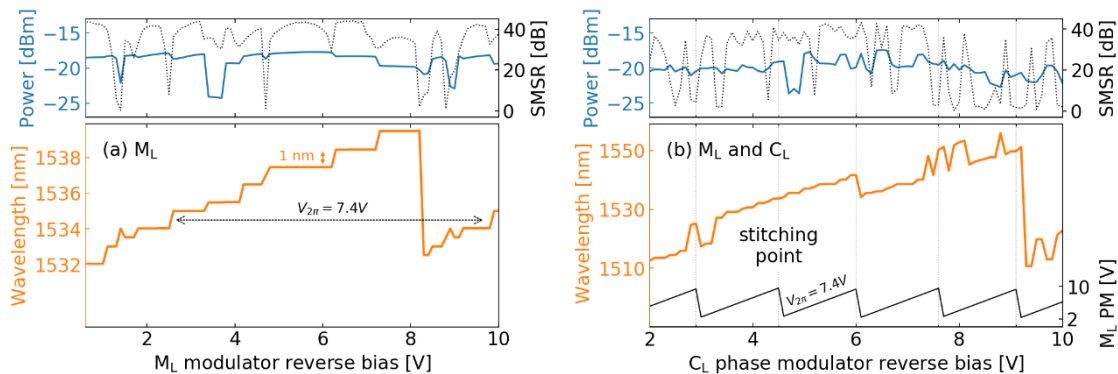


Figure 3 Lasing wavelength, power and side mode suppression ratio (SMSR) when (a) only medium phase modulator is biased (b) coarse and medium filters are biased in synchrony. $I_{\text{SOA}} = 150$ mA, PM – phase modulator.

Conclusions

To achieve a linear sweep a model of PM absorption and a more accurate measurement of the response of the coarse and medium filters is necessary.

Acknowledgements

This project has received funding from the European Union’s Horizon 2020 research and innovation program under the Marie Skłodowska-Curie grant agreement No. 721766. The data for the group refractive index was provided by Dan Zhao. The filter arm mismatch was calculated based on the laser mask files provided by Sylwester Latkowski.

References

- [1] W. Drexler, M. Liu, A. Kumar, et al., “Optical coherence tomography today: speed, contrast, and multimodality,” *Journal of Biomedical Optics*, vol. 19, no. 7, pp. 071412–071412, 2014.
- [2] S. Latkowski, A. Hänsel, N. Bhattacharya, et al., “Novel widely tunable monolithically integrated laser source,” *IEEE Photonics Journal*, vol. 7, no. 6, pp. 1–9, 2015.
- [3] W. Yao, “Towards a high-capacity multi-channel transmitter in generic photonic integration technology,” 2017.
- [4] D. Pustakhod, K. Williams, and X. Leijtens, “Fast and robust method for measuring semiconductor optical amplifier gain,” *IEEE Journal of Selected Topics in Quantum Electronics*, vol. 24, no. 1, pp. 1–9, 2017.
- [5] D. Zhao, D. Pustakhod, K. Williams, et al., “High resolution optical frequency domain reflectometry for analyzing intra-chip reflections,” *IEEE Photonics Technology Letters*, vol. 29, no. 16, pp. 1379–1382, 2017.
- [6] M. Smit, X. Leijtens, H. Ambrosius, et al., “An introduction to InP-based generic integration technology,” *Semiconductor Science and Technology*, vol. 29, no. 8, p. 083001, 2014.